ELSEVIER

Soil Dynamics and Earthquake Engineering 18 (1999) 423–435

SOIL DYNAMICS AND EARTHQUAKE ENGINEERING

Evidence of nonlinear site response in horizontal-to-vertical spectral ratio from near-field earthquakes

P. Dimitriu[a,*], I. Kalogeras[b], N. Theodulidis[a]

[a]*Institute of Engineering Seismology and Earthquake Engineering, P.O. Box 53 Finikas, GR-55102 Thessaloniki, Greece*
[b]*Geodynamic Institute, National Observatory of Athens, P.O. Box 20048, GR-11810 Athens, Greece*

Received 6 April 1999; accepted 6 April 1999

Abstract

The issue is addressed as to whether the horizontal-to-vertical spectral ratio (HVSR) method is sensitive to the amplitude of ground motion from near-field earthquakes. Twenty-one three-component accelerograms from two closely located similar soil sites in the town of Lefkas are used. The recordings represent 17 earthquakes covering a wide range of magnitudes, epicentral distances and azimuths. Peak horizontal accelerations (PGA) and velocities (PGV) lie in the ranges 20–540 cm/s^2 and 1.4–55.2 cm/s. For each HVS ratio, the site's fundamental-resonance frequency, f_{res}, is determined visually. Linear correlation analysis shows that f_{res} is strongly (negatively) correlated to PGA and PGV (r between -0.7 and -0.8); no correlation is found with resonance amplitude or epicentral distance. We show that the observed correlation is attributable to soil nonlinearity and indicate how weak-motion estimates of f_{res} can be corrected for use in assessing site response during strong shaking.

Keywords: Horizontal-to-vertical spectral ratio; Near field; Fundamental-resonance frequency; Nonlinear site response; Soil nonlinearity; Shear-modulus degradation; Linear correlation

1. Introduction

Assessing sediment response during strong earthquakes is a prime task of engineering seismology. In the absence of detailed geotechnical information, two techniques are usually used to obtain such estimates in situ. The first, known as the standard spectral ratio (SSR) method [1], requires the presence of a so-called "reference" site, i.e. a site with—ideally—a flat spectral response in the frequency band of interest, nearby the soil site (to minimize source and path effects). Then the response (transfer function, TF) of the soil site is approximated by the Fourier spectral ratio of soil- to rock-site recordings. Recent strong earthquakes near important populated centres have produced a large number of good-quality strong-motion recordings from a variety of site conditions (e.g. Loma Prieta, Northridge and Kobe). Subsequent studies of site response have revealed that the SSR depends on shaking intensity (and hence on earthquake magnitude): both the frequency and the amplitude of the fundamental site-resonance peak decrease with increasing intensity (e.g. Refs. [2–6]). This result is interpreted as evidence of soil nonlinearity, due to the degradation of the soil shear modulus with increasing strain level, and agrees with theoretical predictions (e.g. Ref. [7]). More complex nonlinear phenomena have been observed in vibrator-aided field experiments on soft sediment sites [8,9].

In practice, it is seldom possible to find a suitable reference site, as most "rock" sites seem to have a response of their own because of their geology or topography or both (e.g. Refs. [10–16]). Therefore another, non-reference-site technique has become very popular. By this technique, known as the horizontal-to-vertical spectral ratio (HVSR) method, site response (TF) is estimated from the Fourier spectral ratios of the horizontal components of a recording to the vertical one. Despite the apparent failure to correctly assess the amplification level, HVSR has been found to yield reliable estimates of the site resonance frequencies (especially the fundamental one), comparing favourably with other methods and thus finding widespread application (e.g. Refs. [17–22]). A recent study of the Japan Meteorological Agency dataset, consisting of 2166 recordings from 387 events, demonstrated the stability of the HVSR method with respect to earthquake magnitude, distance and depth [23]. It is hence implied that, unlike SSR, HVSR is independent of shaking intensity, although it is recognized that the data are mainly intermediate to far field.

In the present study we examine the possible dependence

* Corresponding author. Tel.: + 30-31-476081; fax: + 30-31-476085.
E-mail address: pedim@itsak.gr (P. Dimitriu)

0267-7261/99/$ - see front matter
PII: S0267-7261(99)00014-7

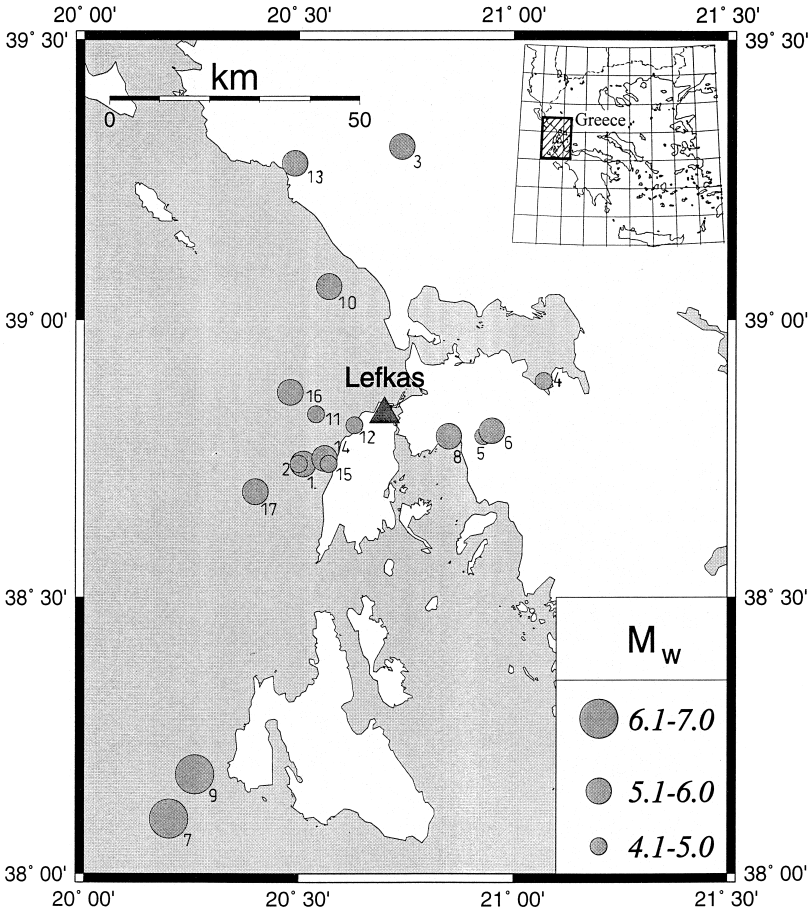

Fig. 1. Map of the study area, showing location of the instrument sites and epicentres of the 17 earthquakes studied. See Table 1.

Table 1
Relevant earthquake data. *R* is epicentral distance; azimuth of epicentres is relative to the recording stations (coordinates: 38.83°N, 20.72°E). Recordings Le3, Le4, etc. and Le83-1, Le83-2, etc. come from the GI-NOA and ITSAK stations, respectively

S. No.	Event date (dd/mm/yy)	Coordinates		M_W	Mechanism	*R* (km)	Azimuth (°N)	Recordings
		(°N)	(°E)					
1	04/11/73	38.74	20.51	5.8	Thrust	21	241	Le4
2	04/11/73	38.74	20.50	5.0		22	242	Le3
3	10/03/81	39.31	20.74	5.8	Thrust	53	2	Le5
4	10/04/81	38.89	21.07	4.7		31	78	Le6
5	25/05/81	38.79	20.93	4.7		19	104	Le7
6	27/05/81	38.80	20.95	5.5		20	99	Le8
7	17/01/83	38.10	20.20	7.0	Str-Slip	93	209	Le83-1
8	23/03/83	38.79	20.85	5.4		12	112	Le83-3
9	23/03/83	38.18	20.26	6.2	Str-Slip	83	209	Le83-4
10	31/08/85	39.06	20.57	5.4		29	333	Le85-1
11	24/04/88	38.83	20.54	5.0		16	270	Le1, Le88-2
12	10/11/92	38.81	20.63	4.8		8	254	Le92-1
13	13/06/93	39.28	20.49	5.9	Thrust	54	338	Le9
14	25/02/94	38.75	20.56	5.6		16	237	Le10, Le94-1
15	27/02/94	38.74	20.57	4.7		16	233	Le11, Le94-2
16	29/11/94	38.87	20.48	5.2		21	282	Le12, Le94-6
17	01/12/94	38.69	20.40	5.1		32	241	Le13

Table 2
PGA and PGV values, frequency (f_{res}) and amplitude (A_{res}) of the HVSR fundamental-resonance peaks for the two horizontal components of the recordings used in the correlation analysis. The second sets of PGV and f_{res} values correspond to original component orientation: 25° E for Le1 and Le9–12 and 25°W for the others (L-component)

Recording	L-comp. (NS)				T-comp. (EW)			
	PGV (cm/s)	f_{res} (Hz)	A_{res}	PGA (cm/s^2)	PGV (cm/s)	f_{res} (Hz)	A_{res}	PGA (cm/s^2)
Le4	**54.5/55.2**	**1.7/2.1**	**7.5**	**540**	**14.2/26.3**	**2.6/3.1**	**5.2**	**243**
Le3	3.2/3.2	3.2/3.4	6.5	52	4.1/4.8	3.7/3.7	8.0	63
Le5	4.4/3.3	2.8/2.8	7.1	55	3.6/4.7	3.2/3.2	5.3	100
Le7	1.6/2.1	3.5/3.2	4.9	55	1.9/1.4	3.9/3.6	5.9	25
Le8	*5.6/4.7*	*3.1/3.0*	*6.0*	*84*	*3.1/4.2*	*3.1/3.3*	*7.6*	*120*
Le1	**9.2/7.6**	**2.4/3.0**	**7.8**	**171**	**12.9/13.9**	**2.8/2.5**	**13.7**	**190**
Le9	*5.8/7.4*	*3.0/2.9*	*8.0*	*116*	*5.0/2.2*	*3.0/2.9*	*6.0*	*83*
Le10	**17.8/13.4**	**2.0/1.8**	**5.4**	**194**	**6.6/13.4**	**2.9/2.8**	**4.3**	**146**
Le11	2.2/3.1	4.1/3.8	5.0	64	3.8/2.9	4.0/4.0	6.7	88
Le12	3.4/3.2	3.4/3.0	4.6	74	4.7/4.9	3.1/3.0	7.4	91
Le6	1.4	3.8	7.0	27	1.3	3.7	8.8	31
Le13	1.9	3.6	3.7	27	1.5	3.8	3.7	36
Le83.1	*6.1*	*2.8*	*7.0*	*59*	*6.6*	*2.8*	*6.5*	*62*
Le83-3	3.2	2.7	6.7	45	3.7	3.0	8.9	42
Le83-4	2.4	3.5	8.0	22	2.2	3.5	8.0	26
Le85-1	2.2	3.5	5.5	52	4.1	3.5	8.0	79
Le88-2	**14.6**	**2.5**	**11.0**	**230**	**4.9**	**3.2**	**5.0**	**93**
Le92-1	*5.1*	*2.8*	*10.0*	*106*	*4.2*	*3.2*	*7.8*	*76*
Le94-1	**14.6**	**2.0**	**6.0**	**165**	**7.2**	**2.0**	**4.0**	**100**
Le94-2	1.7	3.3	7.5	45	2.0	3.2	7.0	36
Le94-6	4.2	3.5	5.8	68	3.3	3.5	5.5	47

of HVSR on ground-motion amplitude by using 21 three-component accelerograms recorded by two analogue stations located on nearby similar soil sites in the town of Lefkas (Lefkas Island, Ionian Sea). The recordings cover the time period November 1973–December 1994 and correspond to 17 earthquakes with M_w magnitude from 4.7 to 7.0 and epicentral distance from 8 to 93 km (only two >54 km). The recorded PGA lies in the range 20–540 cm/s^2. Regardless of instrument orientation, we find very strong negative correlation (r between about −0.7 and −0.8) between the soil's fundamental resonance frequency and the recorded PGA and PGV. We show that soil nonlinearity can explain this correlation.

2. Earthquake and strong-motion data

The strong-motion dataset used consists of 21 three-component accelerograms from two permanent analogue (SMA-1) stations in the town of Lefkas, on Lefkas Island in the Ionian Sea (Fig. 1). One station belongs to the Geodynamic Institute of the National Observatory of Athens (GINOA) and the other to the Institute of Engineering Seismology and Earthquake Engineering (ITSAK), Thessaloniki. The two stations are installed on the ground floors of two stiff buildings located on nearby (about 150 m apart) soil sites, composed of 8–12 m of sandy-silt ($V_S = 70–100$ m/s) overlying marl ($V_S \approx 600$ m/s) [24]. The recordings cover the time period November 1973–December 1994 and correspond to 17 earthquakes with M_w magnitude from 4.7 to 7.0 and epicentral distance from 8 to 93 km (Table 1). The focal depths do not exceed 20 km. As can be seen from Table 1, the earthquakes cover a wide range of magnitudes, epicentral distances and azimuths to the recording stations. All but two of them can be regarded as near field events, as their epicentral distances do not exceed 54 km. The recorded peak horizontal accelerations (PGA) and velocities (PGV) also lie in a wide range, 22–540 cm/s^2 and 1.4–55.2 cm/s (Table 2).

As expected, the biggest differences between the two horizontal components, both in terms of peak values and waveform, occur in the four strongest recordings (bold type in Table 2). This is a consequence of the source (mechanism and directivity) effect as a result of the proximity and size of the corresponding earthquakes. In the other recordings the differences are less pronounced.

3. Method

The original analogue accelerograms were processed following a standard procedure. Thus, they were first digitized, automatically or manually, and then instrument and baseline corrected. The high-pass and low-pass filters were typically set at 0.1–0.4 Hz and 25–27 Hz, respectively. As a result, digitized acceleration, velocity and displacement data were obtained. The recordings were then rotated so that the L-component has NS orientation

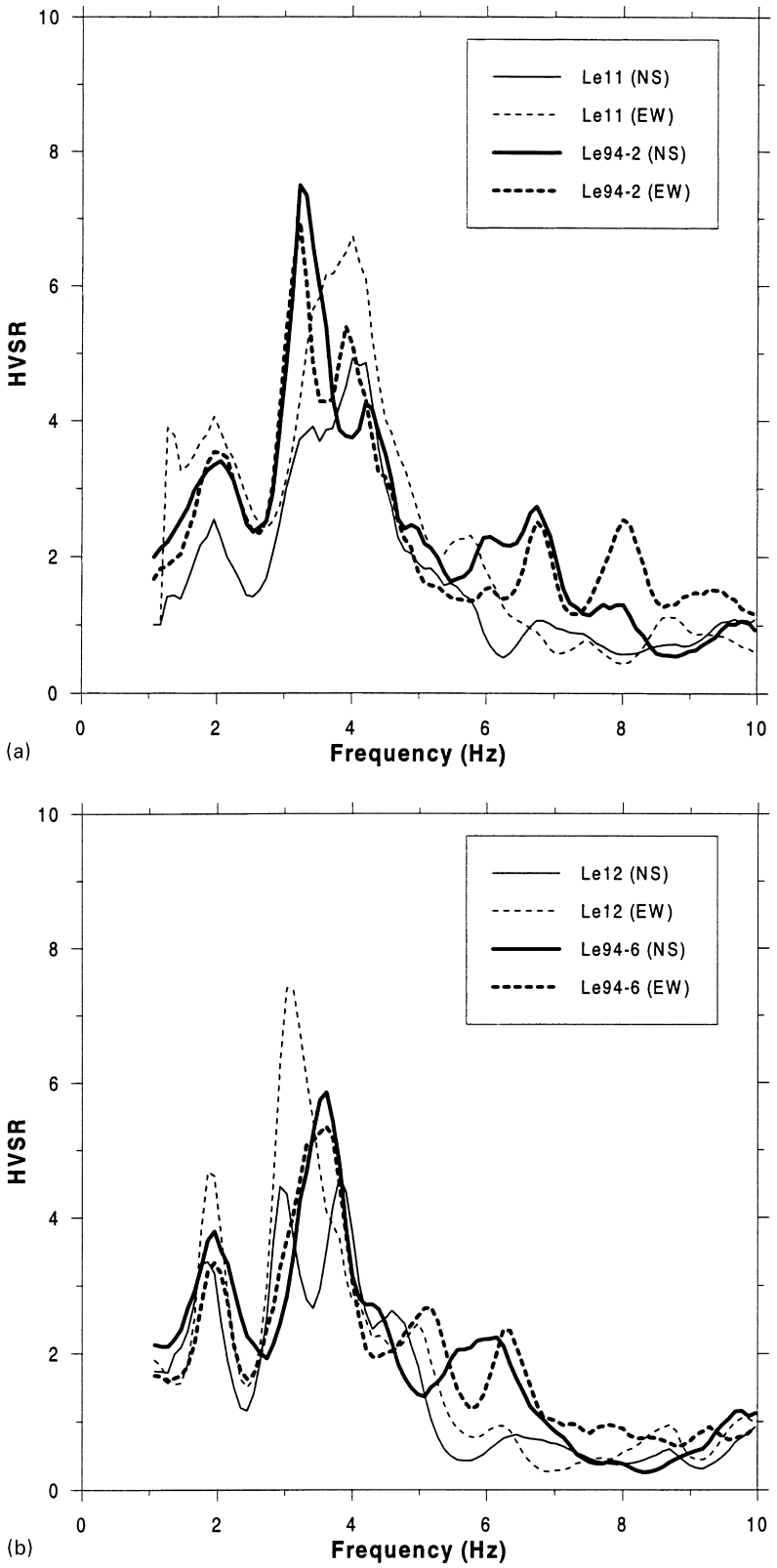

Fig. 2. HVSR at the two instrument sites from the same event: (a) event 15 ($M_w = 4.7$); and (b) event 16 ($M_w = 5.2$). Thick/thin lines: ITSAK/GI-NOA recordings. See Tables 1 and 2.

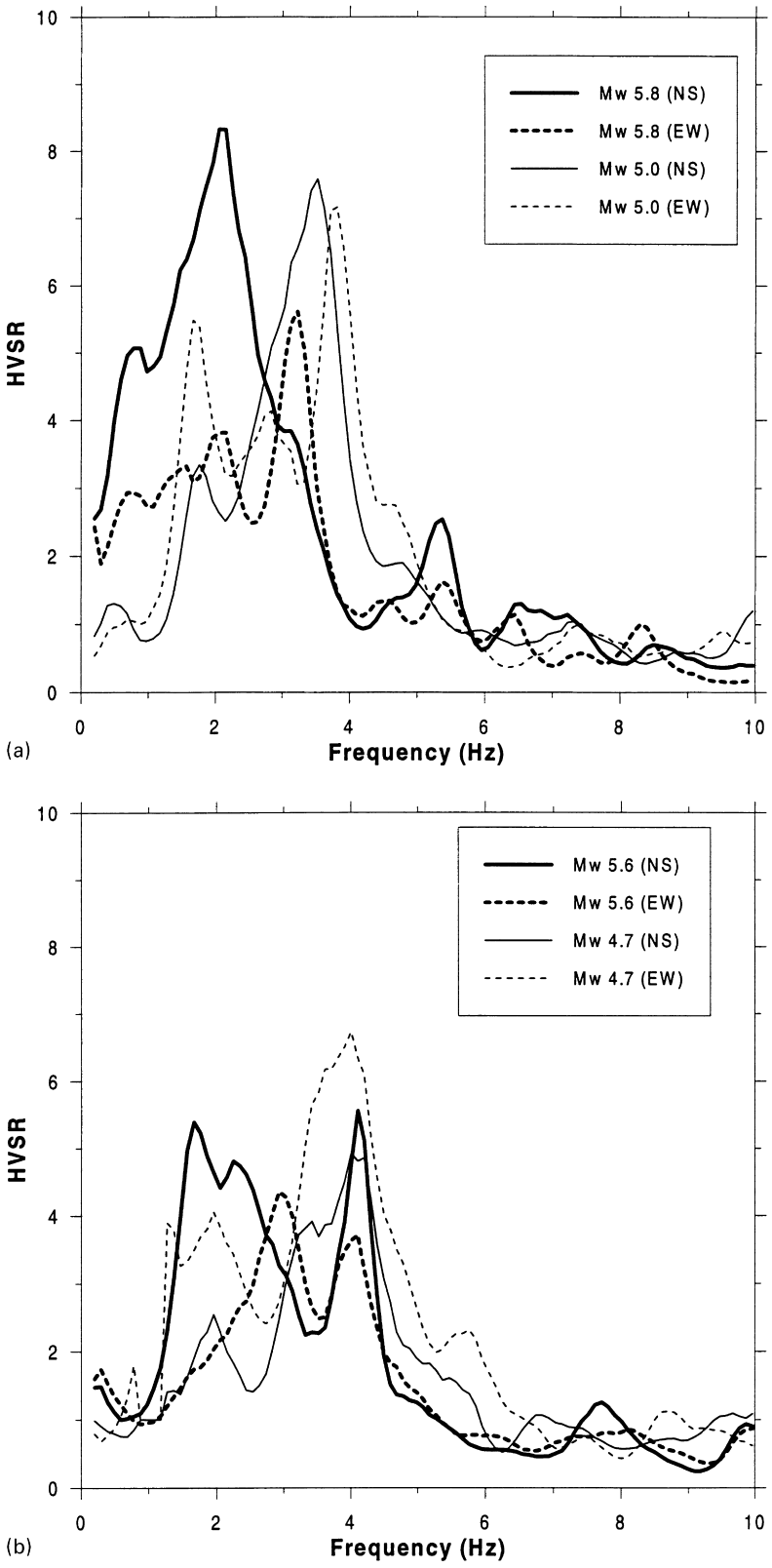

Fig. 3. HVSR from two mainshock–aftershock pairs: (a) $M_w = 5.8$ (Le4) and $M_w = 5.0$ (Le3); (b) $M_w = 5.6$ (Le10) and $M_w = 4.7$ (Le11). Thick/thin lines: mainshocks/aftershocks. See Tables 1 and 2.

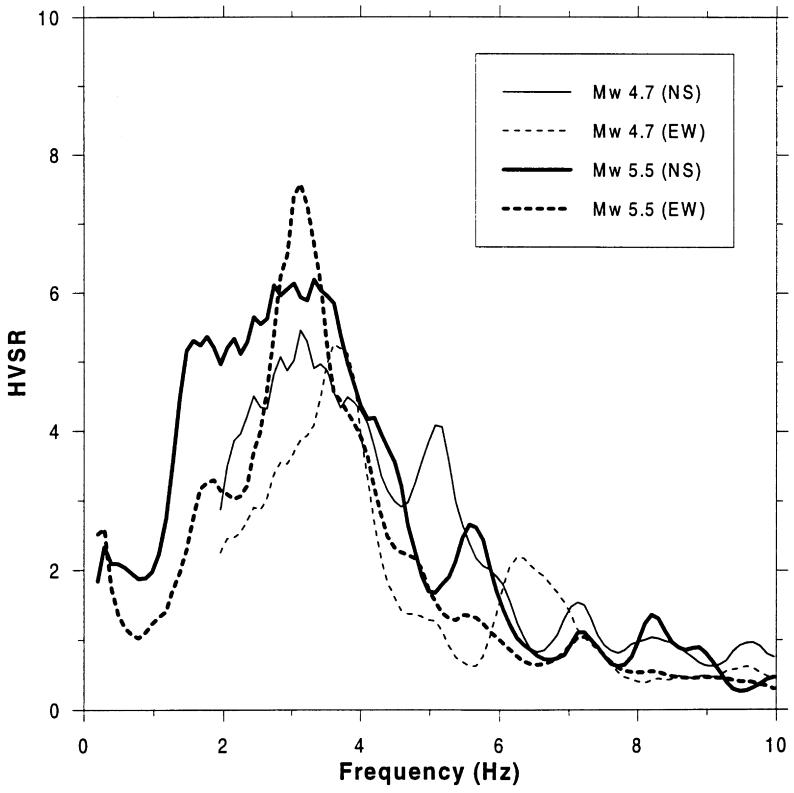

Fig. 4. Same as Fig. 3 but for a foreshock–mainshock pair: $M_w = 4.7$ (Le7) and $M_w = 5.5$ (Le8).

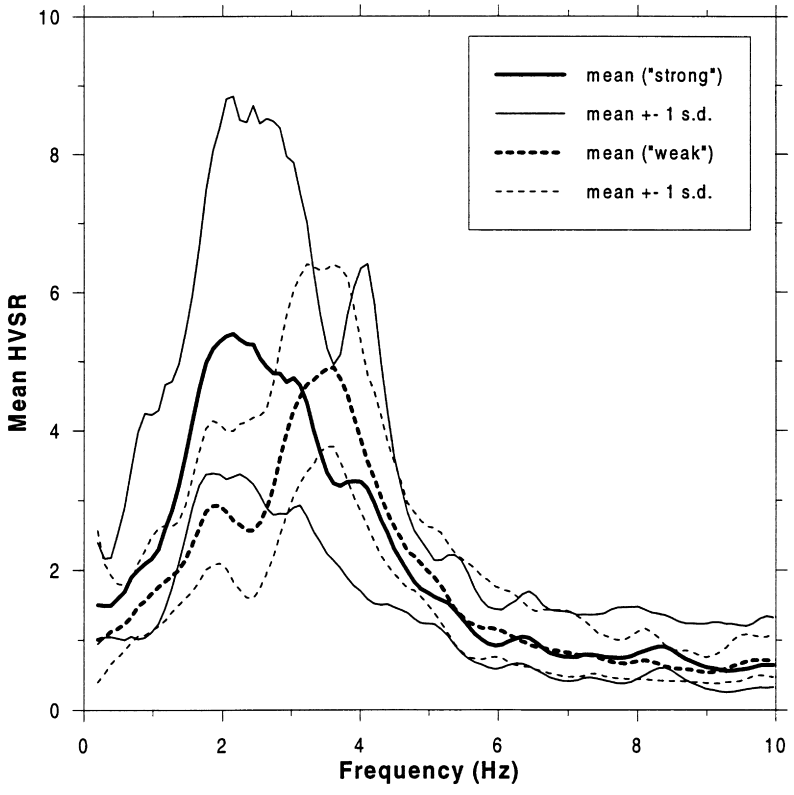

Fig. 5. Mean empirical HVSR for comparatively stronger and weaker ground motion (recordings with PGV $>$ 7 cm/s and PGV $<$ 5 cm/s, respectively; see Table 2). Continuous/dashed lines: stronger/weaker ground motion; thick/thin lines: mean/mean ± 1 standard deviation values.

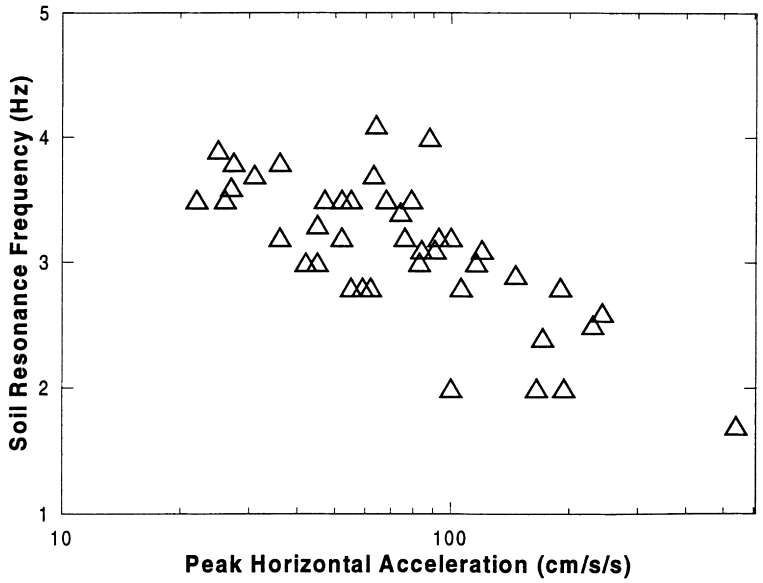

Fig. 6. Correlation between variables (f_{res}, PGA) (see Table 3).

and the T-component has EW orientation. To check for possible dependence on direction of ground motion, unrotated recordings were also used (see Table 2). Fourier spectra of the three components of acceleration were then obtained from the first 10.24 s of the recordings, comprising the strongest (S-wave) arrivals. The spectra were smoothed by using a 0.5 Hz triangular window—a common procedure (e.g. Ref. [22]). The fixed traces of the recordings were processed in the same fashion and were used as noise. HVSR were then computed by taking the ratio between the (smoothed) Fourier spectrum of each horizontal component and the spectrum of the vertical component, but only for those spectral components with amplitude at least three times the corresponding noise amplitude. The frequency and amplitude of the site's fundamental resonance (f_{res} and A_{res}) were determined visually from HVSR: the highest-amplitude peak or the lowest-frequency peak in the few cases where two peaks of similar amplitude occurred was considered. For broad peaks, the frequency of their middle point was taken.

4. Results

4.1. HVSR

Here we present HVS ratios of selected recordings. The first goal is to illustrate the similarity of the ratios from the two station sites (Fig. 2). This similarity, especially from different events, implies similarity of site conditions, which is expected, given the proximity of the two sites and the geology and topography of the area. On the other hand, one can clearly see striking differences between HVSR from two events with similar location but different magnitude, a mainshock and an aftershock (Fig. 3) and a foreshock and a mainshock (Fig. 4). Most importantly, the fundamental site-resonance peaks are clearly shifted toward lower frequencies in the spectra from the stronger shocks, as is also illustrated in Fig. 5, showing the mean HVSR computed for comparatively stronger (PGV $>$ 7 cm/s) and weaker (PGV $<$ 5 cm/s) ground motion. This suggests a possible correlation between the site's fundamental-resonance frequency and quantities characterizing the severity of shaking, such as PGA and PGV.

4.2. Correlation analysis

Figs. 6 and 7(a) are plots of the fundamental-resonance frequency of the site (f_{res}), determined visually for each horizontal component from the HVSR curves, versus the corresponding PGA or PGV value (see Table 2). Linear correlation analysis shows that there is very strong negative correlation between the two pairs of variables (Table 3). Correlation with peak velocity is considered more significant, as horizontal ground velocity is directly related to shear strain. In Table 3 we also show how the statistics of the correlation (f_{res}, PGV) improve after removing the highest PGV value (54.5 cm/s, recording Le4; see Table 2). To investigate the dependence of the correlation on the direction of ground motion, we redid the analysis using 10 recordings with their original component orientation (see Table 2). The obtained correlation is readily improved by removing the two points corresponding to the strongest recording, Le4 (Fig. 7(b) and Table 3). The fundamental-resonance frequency, f_{res}, is found to be uncorrelated to the amplitude of the HVSR fundamental-resonance peak, A_{res} (see Table 2) ($r = -0.114$, $t = -0.92$), as well as to epicentral distance ($r = 0.058$, $t = 0.23$).

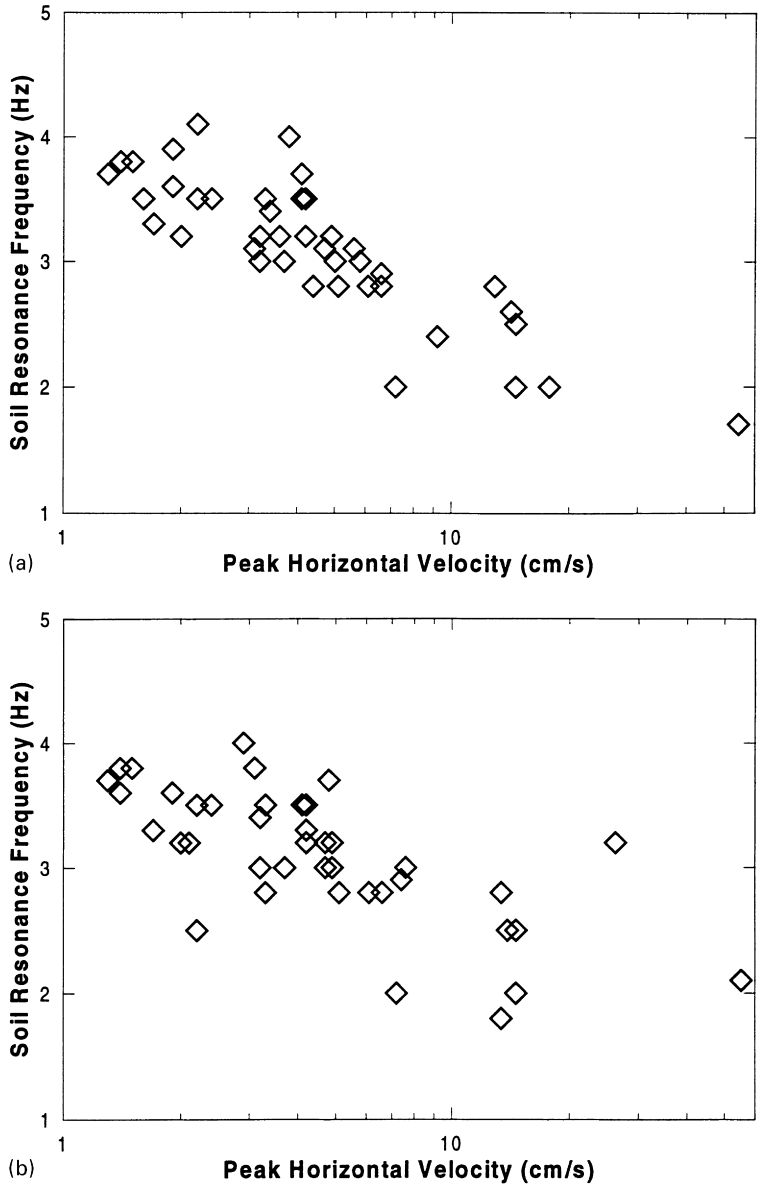

Fig. 7. Correlation between variables (f_{res}, PGV): (a) NS, EW orientation of the L- and T-components; (b) 10 recordings with original orientations (see Tables 2 and 3).

Table 3
Results of linear correlation analysis between the site's fundamental-resonance frequency (f_{res}) and the corresponding PGA and PGV values (Table 2). DF is the number of degrees of freedom (= 40 when all 42 components are used); r is the correlation coefficient and S_r its standard error; t is Student's t-test statistic; r(5%) and t(5%) are the values at the 5% confidence level. Row 3 shows the result of removing the highest PGV value. Rows 4 and 5 correspond to ten recordings taken with their original orientation (see Table 2), respectively with all data and after removing the biggest recording, Le4

Variables	DF	r	r(5%)	S_r	t	t(5%)
f_{res}, PGA	40	−0.703	−0.304	0.112	−6.26	−2.021
f_{res}, PGV	40	−0.694	−0.304	0.114	−6.10	−2.021
f_{res}, PGV	39	−0.789	−0.308	0.098	−8.02	−2.023
f_{res}, PGV (orig.)	40	−0.533	−0.304	0.134	−3.99	−2.021
f_{res}, PGV (orig.)	38	−0.765	−0.312	0.105	−7.32	−2.024

4.3. Theoretical modeling

Here we present the results of linear one-dimensional modeling of HVSR and TF for the Lefkas-site soil structure.

Table 4
Site structure used in linear one-dimensional modeling (Fig. 8) (adapted from Theodulidis and Tsakalidis [24]). Two extreme values of the layer V_S, 100 and 70 m/s, were used (Layer 1 and Layer 2, respectively). Also, more realistic Q values for the marl layer were assumed than those proposed in the reference

	H (m)	Density (kg/m^3)	V_S (m/s)	Q_S	V_P (m/s)	Q_P
Layer 1	8	1900	100	17	170	30
Layer 2	8	1900	70	10	170	30
Halfspace	∞	2200	600	50	1080	120

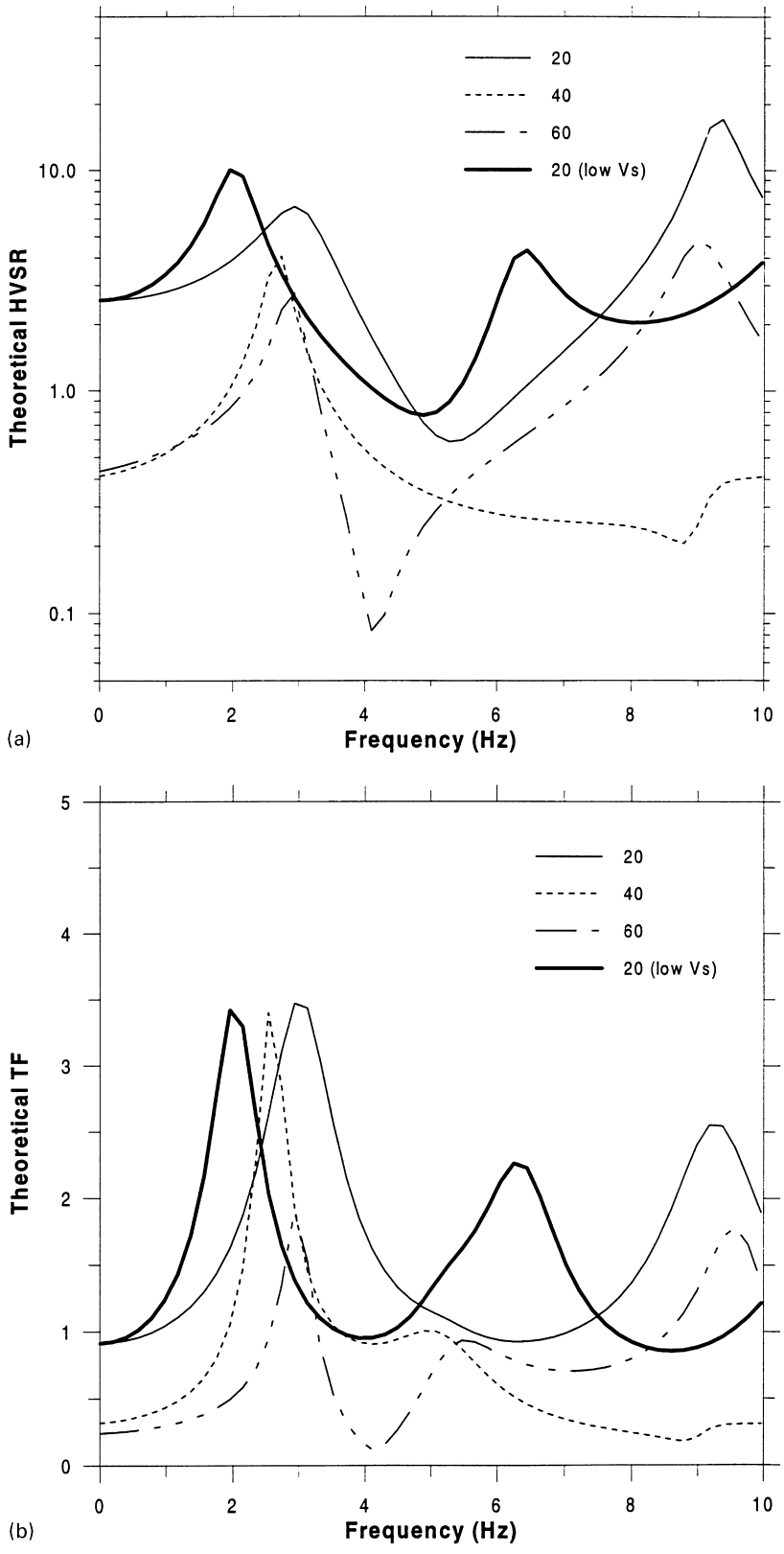

Fig. 8. Theoretical SV-wave modeling of (a) HVSR and (b) TF (relative to bedrock outcrop) for the site structures of Table 4. Thin lines: soil with $V_S = 100$ m/s and incidence at the layer–halfspace interface at 20° (continuous lines), 40° (dashed lines) and 60° (dash-dotted lines) from the vertical. Thick lines: soil with $V_S = 70$ m/s and incidence at 20°.

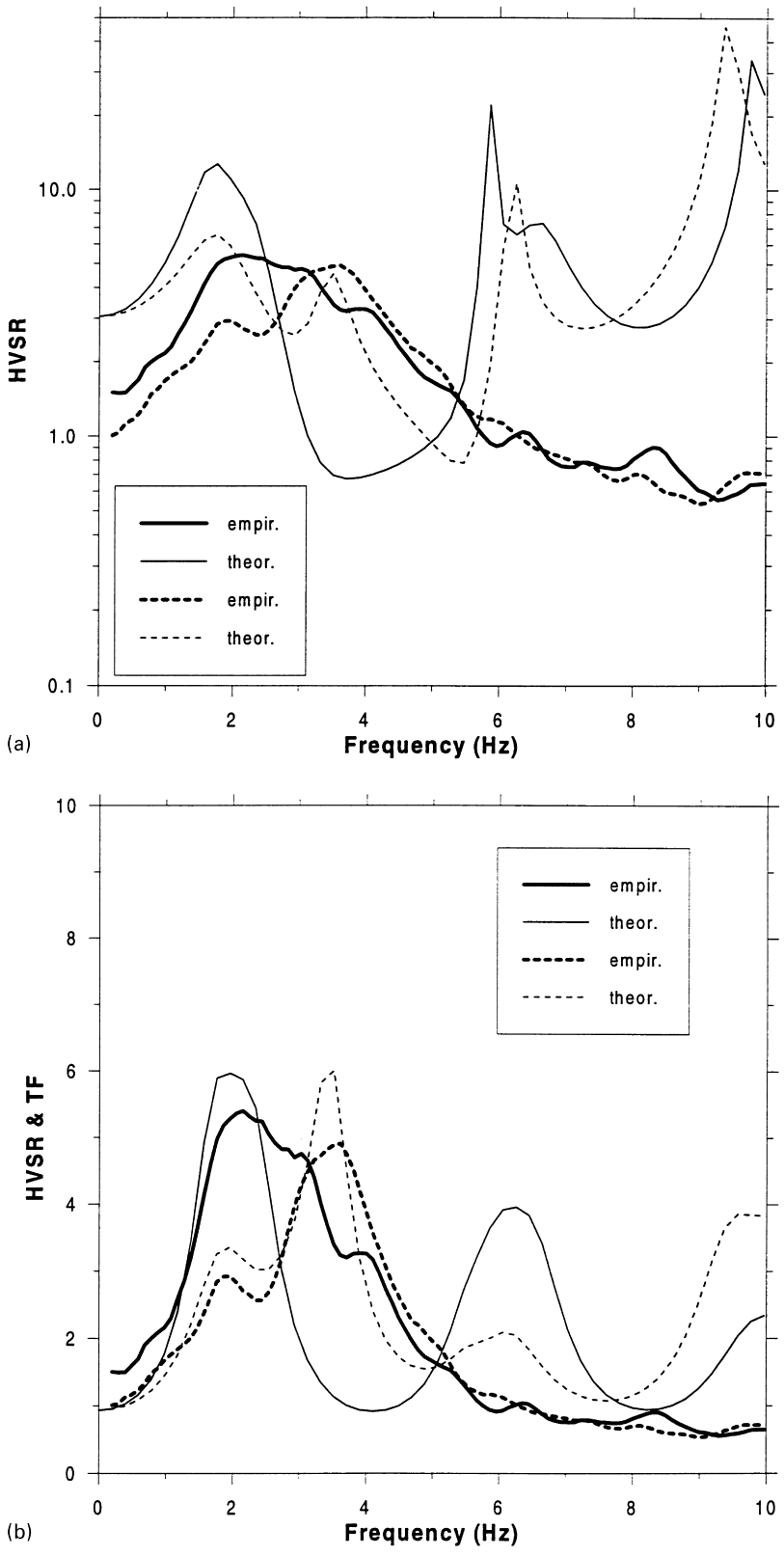

Fig. 9. Mean empirical HVSR for comparatively stronger (PGV $>$ 7 cm/s) and weaker (PGV $<$ 5 cm/s) ground motion (thick dashed and continuous lines, respectively; see Fig. 5) vs. (a) theoretical SV-wave HVSR and (b) TF (relative to bedrock outcrop) (thin lines). Theoretical curves computed for an incidence angle of 20° from the vertical to the soil/bedrock interface for the site structure of Table 5, with the two extreme V_S values for Layer 1: 110 m/s (dashed lines) and 70 m/s (continuous lines).

Table 5
New site structure used in linear one-dimensional modeling (Fig. 9). It was found that $V_S = 110$ m/s gives a "weak motion" fundamental-resonance frequency very close to the observed one (about 3.6 Hz, Fig. 5). Halfspace-parameter values are arbitrary, taken sufficiently high to ensure a strong contrast with the marl layer

	H (m)	Density (kg/m^3)	V_S (m/s)	Q_S	V_P (m/s)	Q_P
Layer 1-1	8	1900	110	17	170	30
Layer 1-2	8	1900	70	10	170	30
Layer 2	75	2200	600	50	1080	120
Halfspace	∞	2500	2000	200	4000	400

TF is defined as the free-surface motion of the layered site versus the free-surface motion of the bedrock outcrop. We used Kennett's reflectivity coefficient method (see Ref. [25]), more specifically an adapted implementation developed at LGIT/IRIGM, Grenoble. The method operates in the frequency domain and uses as input any type of body wave (P, SV or SH) incident at an arbitrary angle to the one-dimensional model of the soil structure studied (soil parameters required are those shown in Table 4). The output comprises the (complex or real) TF of the site (two options: TF relative to any interface within the deposit or relative to the free bedrock surface) and the ratio between the spectra of the horizontal and vertical components (HVSR) on soil surface (only for an obliquely incident P- or SV-wave).

The purpose of the modeling was twofold. First, we sought confirmation that the empirical HVSR are representative of the site response (TF). And second, we wished to determine whether the decrease in the site's fundamental-resonance frequency observed between the comparatively stronger (PGV $>$ 12.8 cm/s) and weaker (PGV $<$ 2.5 cm/s) ground motion (ca. 1.3 Hz, see Fig. 7(a)) was compatible with a realistic change in the shear-wave velocity of the sandy-silt layer. The layer and halfspace parameters used in the linear one-dimensional modeling are listed in Table 4. The SV-wave theoretical HVSR and TF are plotted in Fig. 8 for different incidence angles (from the vertical) and for the two extreme values of the layer V_S (Table 4). The incidence angles were chosen such as to correspond to waves arriving from local and more distant events.

A closer inspection of Fig. 5 reveals that there is a slight indication in the weaker-motion (dashed) curve of another resonance at around 2 Hz, which is absent from the theoretical curves (Fig. 8). There is a strong possibility that this resonance is associated with a marl layer, which in the above oversimplified site structure is assumed to be the halfspace. Indeed, substitution in the formula for the frequency of the fundamental layer resonance, $f_{res} = V_S/4H$, of the values $f_{res} = 2$ Hz and $V_S = 600$ m/s gives $H = 75$ m for the marl layer. In Fig. 9 we compare the average empirical HVSR data of Fig. 5 with the theoretical HVSR and TF computed using the modified site structure (Table 5).

5. Discussion and conclusion

Our results strongly suggest that the fundamental-resonance frequency (f_{res}) of soft-sediment sites, as

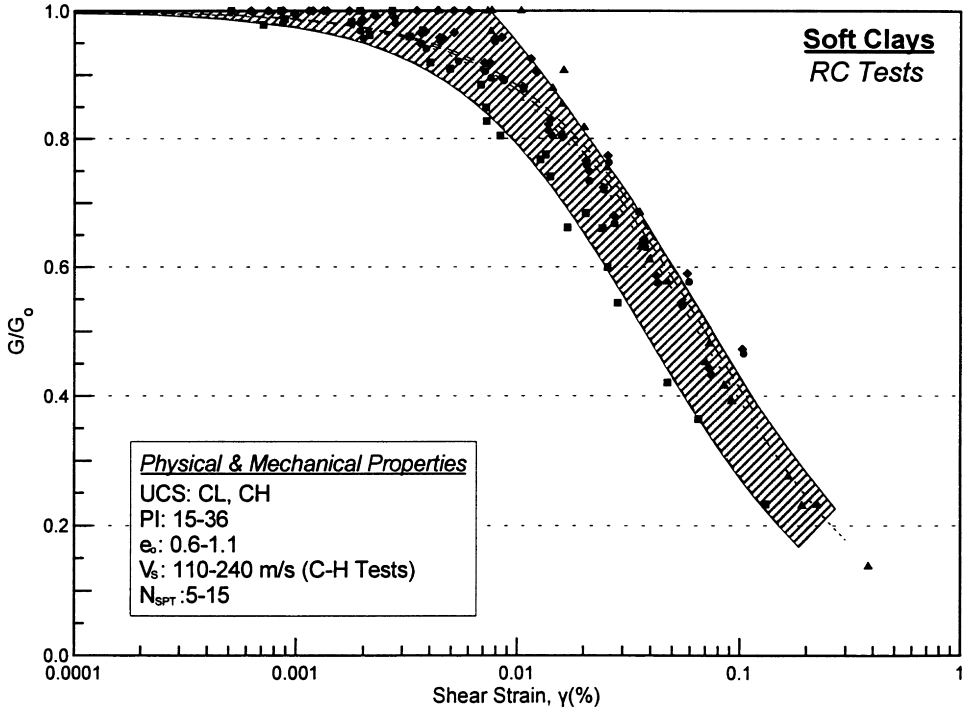

Fig. 10. $G/G_0 - \gamma$ data, from Resonant Column (RC) Tests, for typical Greek soft clays (physical and mechanical properties indicated). Adapted from Anastasiadis [28].

displayed in HVSR, is sensitive to the intensity of shaking from near-field earthquakes. A rich strong-motion dataset is used consisting of 21 three-component accelerograms from 17 (all but two near field) earthquakes covering a wide range of magnitudes, epicentral distances and azimuths (Table 1) as well as peak horizontal accelerations and velocities (Table 2). A strong negative correlation is found between f_{res} and PGA and PGV (Figs. 6 and 7 and Table 3). Correlation with PGV is considered more significant, as horizontal ground velocity is directly related to shear strain. The correlation is stable with respect to the direction of ground motion (Fig. 7). The fact that the correlation is improved by removing the data corresponding to the strongest recording (Table 3) can be attributed to source effects affecting it, thanks to the large size ($M_w = 5.8$) and proximity (21 km) of the earthquake. As may have been expected, owing to the known failure of HVSR to accurately represent amplification level, no correlation is established between f_{res} and the corresponding amplitude of the HVSR peak, A_{res} (Table 3).

Very importantly, no correlation is found between f_{res} and epicentral distance ($r = 0.058$), enforcing our conclusion that the observed behaviour is mainly due to the nonlinear response of the sandy-silt (top) layer. Indeed, separation of ground motion into comparatively "weak" (PGV < 2.5 cm/s) and "strong" (PGV > 12.8 cm/s) motion permits to relate the corresponding resonance-frequency drop of about 1.3 Hz (3.5–2.2 Hz, see Fig. 7(a)) to a realistic degradation of the soil shear modulus (G_s/G_w). Thus, the shear-wave fundamental-resonance frequency of a layer is $f_{res} = V_S/4H$ where H is the layer thickness, and replacing $V_S = (G/\rho)^{1/2}$ gives the following relation between the resonance-frequency shift and modulus change: $\Delta f = f_{res}{}^{w}[1 - (G_s/G_w)^{1/2}]$. Substituting $\Delta f = 1.3$ Hz, $f_{res}{}^{w} = 3.5$ Hz (see Fig. 7) yields $G_s/G_w = 0.4$. Modulus degradation of this magnitude is possible in very soft soils, such as the sandy-silt layer under the Lefkas stations (Table 5), especially at high strain levels. Indeed, the shear strains developed in the layer during the "strong" motions (PGV > 12.8 cm/s) can be estimated from the ratio PGV/V_S. According to Schnabel et al. [26] and Satoh et al. [27], an "effective" shear strain (0.65 of the maximum strain) is more representative of the nonlinear behaviour of soils. Substituting the values 15 cm/s and 70 m/s for PGV and V_S, respectively, and multiplying by 0.65 gives an effective shear strain of about 1.4×10^{-3}. This high strain justifies the above estimate of modulus degradation ($G_s/G_w = 0.4$) as it agrees with $G/G_0 - \gamma$ data (from Resonant Column Tests) for typical Greek soft clays ([28], Fig. 10). Similar values can be found in the international bibliography for cohesive soils (e.g. Refs. [29–31]).

Theoretical (linear) computations confirm the above results. Indeed, taking the two extreme values of V_S in the sandy-silt layer (Table 5) gives a resonance-frequency shift of about 1.1 Hz (Figs. 8 and 9(b))—a value within the range of the empirically observed shifts, 1–1.3 Hz (Figs. 5 and 7(a)). The empirical HVSR being approximated better by the theoretical TF than by the theoretical HVSR (Fig. 9) is not unusual (e.g. Ref. [22]). As far as we know, no explanation of this observation has been proposed. The closest agreement between empirical and model results is obtained for an SV-wave incidence angle of 20° from the vertical at the soil/bedrock interface. This somewhat small angle, for local shallow earthquakes, suggests that the actual soil structure may be deeper and more complex than its model of Table 5. Still, the obviously oversimplified soil model clearly captures the principal soil resonances (see Fig. 9(b)).

Nonlinear site response has been observed and studied by other researchers (e.g. Refs. [2–6]). The novelty of our work is that, unlike those studies, where soil/rock surface (SSR method) or surface/downhole spectral ratios are used to characterize site response, we employ a very popular non-reference-site technique—the HVSR. Moreover, we know of no reports of statistically significant correlation between the empirically evaluated fundamental-resonance frequency of a soil site and a strong-motion parameter.

Mohammadioun [32] discusses the presence of very high vertical accelerations on alluvial sites. He presents data from the 1995 Kobe earthquake where vertical accelerations exceed the horizontal ones in a wide range of frequencies (above 3 Hz and, less pronouncedly, between 0.3 and 0.6 Hz) and ascribes this phenomenon to nonlinear soil behaviour, in particular to the different influence of nonlinearity on compressional and shear waves. Our results support the author's conclusion that nonlinearity must affect the HVSR, indicating the nature and extent of the nonlinear effects. But in contrast to Kobe, only above about 5 Hz do the vertical accelerations in our data become comparable with the horizontal ones (Fig. 5). The somewhat "anomalous" Kobe data may be due to a number of factors, including the mechanism and size of the earthquake, its proximity to the recording stations and the specific seismotectonic and geologic conditions.

In conclusion, our study provides clear evidence that the HVSR method is sensitive to the amplitude of ground motion, as displayed in the strong negative correlation between the site's fundamental-resonance frequency and the strong-motion parameters peak ground velocity and acceleration. An important practical implication of this result is that weak-motion estimates of resonance frequencies of soil sites from HVSR data must be corrected if they are to be used to assess site response during strong shaking. Our study indicates how to make such corrections by making use of $G/G_0 - \gamma$ curves of the soils with the most important contribution to the nonlinear response of a site. It is premature, though, to generalize our results: further research is needed to cover diverse site and seismotectonic conditions.

Acknowledgements

We thank the anonymous reviewers for their valuable

comments and suggestions. We are grateful to P.-Y. Bard for providing the computer code we used in the modeling. P. Hatzidimitriou read the manuscript and made useful remarks. P. Triandaffilidis supplied Fig. 1 and A. Anastasiadis Fig. 10 and relevant references.

References

[1] Borcherdt RD. Effects of local geology on ground motion near San Francisco Bay. Bull Seism Soc Am 1970;60:29–61.
[2] Jarpe SP, Cramer CH, Tucker BE, Shakal AF. A comparison of observations of ground response to weak and strong ground motion at Coalinga, California. Bull Seism Soc Am 1988;78:421–435.
[3] Darragh RB, Shakal AF. The site response of two rock and soil station pairs to strong and weak ground motion. Bull Seism Soc Am 1991;81:1885–1899.
[4] Beresnev IA, Wen KL. Nonlinear soil response—a reality? Bull Seism Soc Am 1996;86:1964–1978.
[5] Field EH, Johnson PA, Beresnev IA, Zeng Y. Nonlinear ground-motion amplification by sediments during the Northridge earthquake. Nature 1997;390:599–602.
[6] Beresnev IA, Atkinson GM, Johnson PA, Field EH. Stochastic finite-fault modeling of ground motions from the Northridge California, earthquake. II. Widespread nonlinear response at soil sites. Bull Seism Soc Am 1998;88:1402–1410.
[7] Yu G, Anderson JG, Siddharthan R. On the characteristics of nonlinear soil response. Bull Seism Soc Am 1992;83:218–244.
[8] Dimitriu PP. Self-modulation and recurrence phenomena in vibrator-induced, steady-state sinusoidal ground vibration. Phys Earth Planet Inter 1988;50:74–82.
[9] Dimitriu PP. Preliminary results of vibrator-aided experiments in nonlinear seismology conducted at Uetze, FRG. Phys Earth Planet Inter 1990;63:172–180.
[10] Cranswick E. The information content of high-frequency seismograms and the near-surface geologic structure of hard rock recording sites. Pageoph 1988;128:335–363.
[11] Sanchez-Sesma FJ, Campillo M. Diffraction of P, SV and Rayleigh waves by topographic features: a boundary integral formulation. Bull Seism Soc Am 1991;81:2234–2253.
[12] Steidl JH, Tumarkin AG, Archuleta RJ. What is a reference site? Bull Seism Soc Am 1996;86:1733–1748.
[13] Boore DM, Joyner WB. Site amplification for generic rock sites. Bull Seism Soc Am 1997;87:327–341.
[14] Chavez-Garcia FJ, Sanchez LR, Hatzfeld D. Topographic site effects and HVSR: a comparison between observations and theory. Bull Seism Soc Am 1996;86:1559–1573.
[15] Spudich P, Hellweg M, Lee WHK. Directional topographic site response at Tarzana observed in aftershocks of the Northridge California, earthquake: implications for mainshock motions. Bull Seism Soc Am 1996;86:S193–S208.
[16] Bouchon M, Baker JS. Seismic response of a hill: the example of Tarzana, California. Bull Seism Soc Am 1996;86:66–72.
[17] Theodulidis N, Bard PY. Horizontal to vertical ratio and geological conditions: an analysis of strong motion data from Greece and Taiwan (SMART-1). Soil Dynam Earthquake Engng 1995;14:177–197.
[18] Theodulidis N, Archuleta RJ, Bard PY, Bouchon M. Horizontal-to-vertical spectral ratio and geological conditions: the case of Garner Valley downhole array in southern California. Bull Seism Soc Am 1996;86:306–319.
[19] Lachet C, Hatzfeld D, Bard PY, Theodulidis N, Papaioannou Ch, Savvaidis A. Site effects and microzonation in the city of Thessaloniki (Greece): comparison of different approaches. Bull Seism Soc Am 1996;86:1692–1703.
[20] Bonilla FL, Steidl JH, Lindley GT, Tumarkin AG, Archuleta RJ. Site amplification in the San Fernando Valley, CA: variability of site effect estimation using the S-wave, coda and H/V methods. Bull Seism Soc Am 1997;87:710–730.
[21] Raptakis D, Theodulidis N, Pitilakis K. Data analysis of the Euro-seistest strong motion array in Volvi (Greece): standard and horizontal-to-vertical spectral ratio techniques. Earthquake Spectra 1998;14:203–224.
[22] Dimitriu PP, Papaioannou ChA, Theodulidis NP. EURO-SEISTEST strong-motion array near Thessaloniki, Northern Greece: a study of site effects. Bull Seism Soc Am 1998;88:862–873.
[23] Yamazaki F, Ansary MA. On the stability of horizontal-to-vertical spectrum ratio of earthquake ground motion. Bull ERS 1997;30:27–44.
[24] Theodulidis N, Tsakalidis K. Site effects on strong ground motion over simple geology structure: the cases of Lefkas and Argostoli (Greece). Proceedings of the XXIV General Assembly of the European Seismological Commission, Athens, 19–24 September, 1994 1994;III:1640–1649.
[25] Kennett BL, Kerry NJ. Seismic waves in stratified halfspace. Geophys J R Astr Soc 1979;57:557–583.
[26] Schnabel PB, Lysmer J, Seed HB. SHAKE: a computer program for earthquake response analysis of horizontally layered sites. Report UCB/EERC 72/12 (1972), Earthquake Engineering Research Center (EERC), University of California, Berkeley.
[27] Satoh T, Sato T, Kawase H. Nonlinear behaviour of soil sediments identified by using borehole records observed at the Ashigara Valley, Japan. Bull Seism Soc Am 1995;85:1821–1834.
[28] Anastasiadis AJ. Contribution to the determination of the dynamic properties of natural Greek soils. PhD Thesis (in Greek), Department of Civil Engineering, Aristotle University of Thessaloniki, 1994 (385 pp).
[29] Sun JI, Golesorchi R, Seed HB. Dynamic moduli and damping ratios of sand and clay. Report UCB/EERC 88/15 (1988), Earthquake Engineering Research Center (EERC), University of California, Berkeley.
[30] Vucetic M, Dobry R. Effect of soil plasticity on cycle response. J Soil Mech Foundations Div, ASCE 1991;117:89–107.
[31] Ishibashi I, Zhang X. Unified dynamic shear moduli and damping ratios of sand and clay. Soils and Foundations 1993;33:182–191.
[32] Mohammadioun B. Nonlinear response of soils to horizontal and vertical bedrock ground motion. J Earthquake Engng 1997;1:93–119.